Coupling of core-edge gyrokinetic simulations coupling and Tungsten impurity transport in JET with XGC

Julien Dominski

Princeton Plasma Physics Laboratory

November 12, 2018

Plan of today presentation

1. **Core-edge coupled simulations**
   1.1 A minimal core-edge coupling scheme [Dominski et al **Phys. Plasmas** 25 (5) 2018]
   1.2 Cross-verification between GENE and XGC [Merlo, Dominski et al **Phys. Plasmas** 25 (6) 2018]
   1.3 Core-edge coupled simulation with GENE-XGC [Dominski, Merlo et al **ECP reports** 2018] (to publish)
2. **Impurities in XGC**
   2.1 Verification of neoclassical physics [Dominski et al **To be submitted** early 2019]
   2.2 Study JET plasma under Tungsten contamination [Dominski et al **Nuclear Fusion** to submit Jan 2019]
   2.3 Atomic physics: ionization/recombination and sputtering
3. **Vision for the incoming years**

A. **Not-discussed today**
   A.1 Collaboration with A. Diallo on ELM physics. [Diallo, Dominski, et al **Physical Review Letters** 2018]
   A.2 New numerical scheme [Dominski et al. *"Gyroaveraging operations using adaptive matrix operators"* **Phys. Plasmas** 2018]

1. Core-edge coupling: motivation

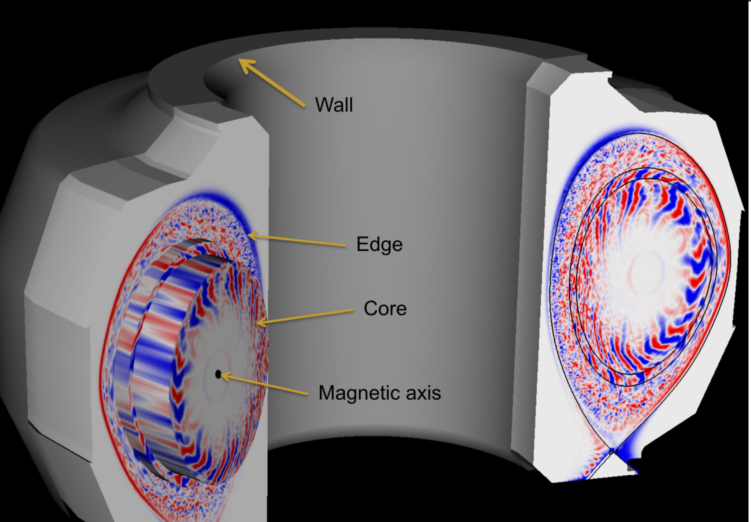

First coupled simulation of turbulence in a Tokamak device.

J. Dominski et al., Physics of Plasmas 25, 072308 (2018)
Visualization : Dave Pugmire (ORNL)

- Simulation of turbulence physics based on first-principles gyrokinetic codes.
- XGC is the leading gyrokinetic code for simulating the edge region.
- GEM and GENE are leading gyrokinetic codes for simulating the core region.

1.1 A core-edge coupling scheme with minimal data move

The gyrocentre distribution function f is evolved with the 5D gyrokinetic equation

$$\frac{\partial f}{\partial t} + \dot{\boldsymbol{X}}[\phi] \cdot \frac{\partial f}{\partial \boldsymbol{X}} + \dot{v}_{\|}[\phi] \frac{\partial f}{\partial v_{\|}} = 0 \tag{1}$$

and the consistent electrostatic potential is solved with the gyrokinetic Poisson Eq.

$$\mathcal{L}\phi = \bar{n}, \tag{2}$$

where the right hand side is computed with

$$\bar{n}(\boldsymbol{x}) = \int_{-\infty}^{+\infty} dv_{\|} \int_{0}^{+\infty} d\mu \oint d\alpha\, f(\boldsymbol{x} - \boldsymbol{\rho}, v_{\|}, \mu). \tag{3}$$

Plus Ampere's law for electromagnetic simulation (later in the coupling project).

1. A composite distribution function is used

$$\delta\check{f} = \varpi\,\delta f^{\mathrm{Core}} + (1-\varpi)\,\delta f^{\mathrm{Edge}}. \qquad (4)$$

Need large enough overlap and enough particles to handle $(f^{\mathrm{Core}} - f^{\mathrm{Edge}}) \cdot \nabla\varpi$.

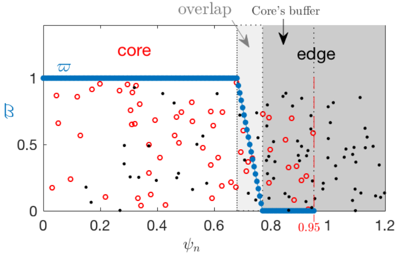

2. The unique field is solved with $\mathcal{L}\check{\phi} = \bar{n}[\check{f}]$.

$$\bar{n} = \int d\boldsymbol{X}\,dv_{\|}\,d\mu\,d\alpha\,\delta(\boldsymbol{X}+\boldsymbol{\rho}-\boldsymbol{x})\left[\underbrace{\varpi(\boldsymbol{X})f^{\mathrm{C}}}_{\text{local in core}} + \underbrace{(1-\varpi(\boldsymbol{X}))f^{\mathrm{E}}}_{\text{local in edge}}\right]. \qquad (5)$$

3. $\bar{n}^{\mathrm{C}}$ is sent to the edge where $\check{\phi}$ is solved and sent back to the core (ADIOS).

4. Both sides push f with the same Vlasov equation $\left(\frac{\partial f}{\partial t} + \dot{\boldsymbol{X}}[\check{\phi}] \cdot \frac{\partial f}{\partial \boldsymbol{X}} + \dot{v}_{\|}[\check{\phi}]\frac{\partial f}{\partial v_{\|}} = 0\right)$.

5. Buffer zone permits to resolve banana orbits of particles crossing the overlap and to delay the propagation of artificial effects due to the core's boundary.

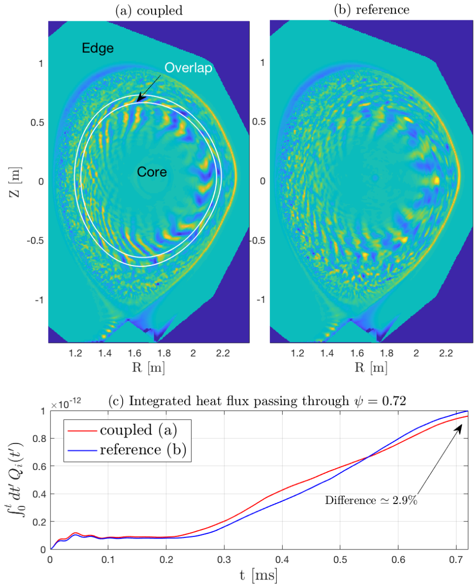

Verification

Two XGC executables, one for the core and one for the edge, are coupled together. (Avoid the grid interpolation issue.)

Test case is a nonlinear turbulent relaxation problem with realistic geometry and pedestal gradients.

Streamers propagate from the edge to the core.

Coupling model has been verified to be accurate within a few percent.

To illustrate the importance of using a unique field, we study a failed case where **two solvers** are used

$$\mathcal{L}^{\mathrm{C}}\phi^{\mathrm{C}} = \bar{n}[\varpi f^{\mathrm{C}} + (1-\varpi)f^{\mathrm{E}}],\ \psi_n \in [0, 0.95] \text{ and } \phi^{\mathrm{C}}|_{\psi_n=0.95} = 0, \tag{6}$$

$$\mathcal{L}^{\mathrm{E}}\phi^{\mathrm{E}} = \bar{n}[\varpi f^{\mathrm{C}} + (1-\varpi)f^{\mathrm{E}}],\ \psi_n \in [0, wall] \text{ and } \phi^{\mathrm{E}}|_{wall} = 0. \tag{7}$$

$\mathcal{L}^{\mathrm{C}}$ and $\mathcal{L}^{\mathrm{E}}$ have different boundary conditions. The electric field in the core and edge will be different. This will lead to a phase-mixing suppression of turbulence.

1.1 Two separate solvers lead to artificial turbulence suppression

The common field must be used in both sides GKE, $\frac{\partial f}{\partial t} + \dot{\boldsymbol{X}}[\phi] \cdot \frac{\partial f}{\partial \boldsymbol{X}} + \dot{v}_{\parallel}[\phi] \frac{\partial f}{\partial v_{\parallel}} = 0.$

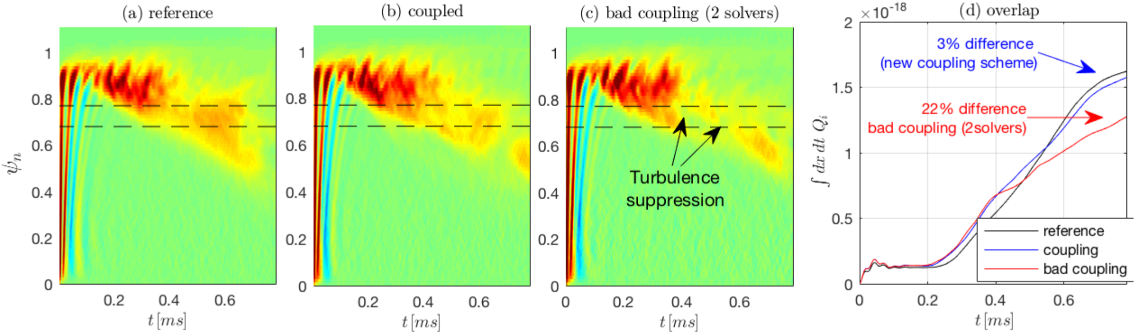

The common field must be used in both sides GKE, $\frac{\partial f}{\partial t} + \dot{\boldsymbol{X}}[\phi] \cdot \frac{\partial f}{\partial \boldsymbol{X}} + \dot{v}_{\parallel}[\phi] \frac{\partial f}{\partial v_{\parallel}} = 0.$

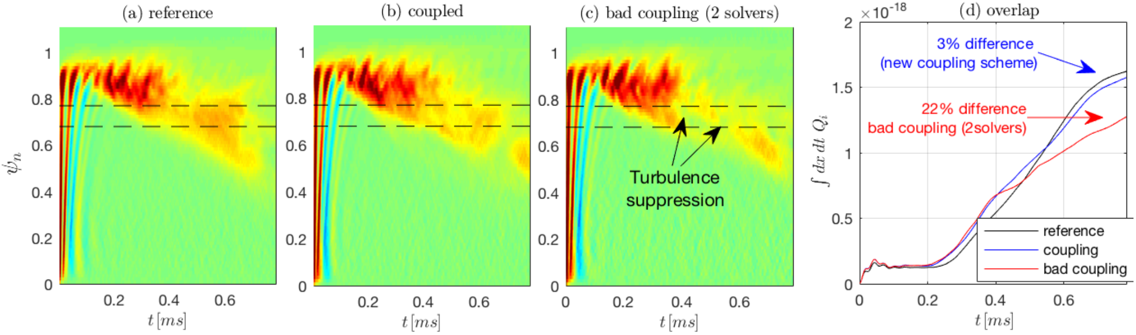

We need the same electrostatic potential to push the same GKE. Is it always enough?

Do we need to exchange more information between core and edge?

Let's look at a simple 1D advection-diffusion of a "blob" from the edge to the core.

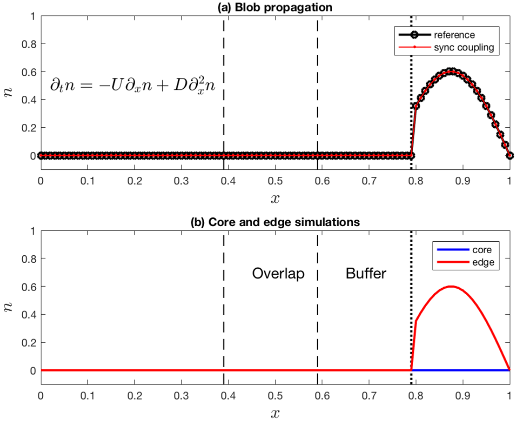

(a) reference (black) and coupled (red) simulations. Dashed lines delimit the overlap.

(b) Core and edge sides of the coupled simulation. Dotted lines delimit the buffer.

The blob does not exists in the buffer at $t = 0$, it needs to be transferred later to the core.

A safe solution is to exchange n (or f) between core and edge buffers every $\sim 10^2 - 10^3$ steps.

Exchange of fluid information might be advantageous, if sufficient and necessary.

Intermediate summary

The use of a core-edge distribution function and a unique field solver permits to couple two codes as if they were one.

Need a large enough overlap width ($>$ turbulence correlation length).

More details in [Dominski et al **Phys. Plasmas** 25 (5) 2018].

Next steps

Simulating more complex plasma (impurities, kinetic electron, flux driven) as discussed.

1.2 Cross-verification between GENE and XGC: first step

Global circular concentric flux surface cross section, CBC gradients, adiabatic electrons.

Linear benchmark

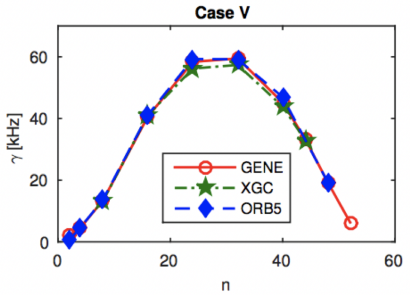

Nonlinear benchmark

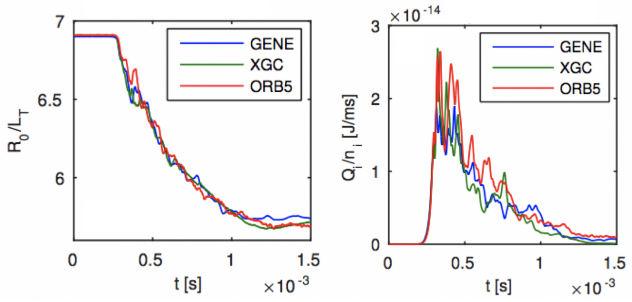

An excellent agreement is found between GENE and XGC. Needed implementation of GENE field-aligned initial condition in XGC.

[Merlo, Dominski et al **Phys. Plasmas** 25 (6) 2018]

The same core-edge coupling scheme used for XGC-XGC has been implemented for coupling GENE (core) and XGC (edge) together.

A new mesh to mesh mapping technique has been implemented for exchanging data between the codes. [Merlo et al., The Sherwood Fusion Theory Conference, Auburn AL, April 2018]

GENE density to XGC grid | **XGC potential to GENE grid**

$$
\begin{tikzcd}
n(x, k_y, z_{\mathrm{GENE}}) \arrow[d] & & \phi(x, k_y, z_{\mathrm{GENE}}) \\
n(x, y, z_{\mathrm{GENE}}) \arrow[d] & & \phi(x, y, z_{\mathrm{GENE}}) \arrow[u] \\
n(x, y, z_{\mathrm{XGC}}) \arrow[d] & & \phi(x, y, z_{\mathrm{XGC}}) \arrow[u] \\
n(R, Z, \varphi) \arrow[dr] & & \phi(R, Z, \varphi) \arrow[u] \\
 & \text{Field solve} \arrow[ur] &
\end{tikzcd}
$$

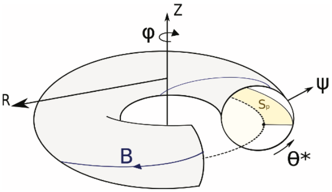

Figure 1: Coordinate systems.

Linear benchmark

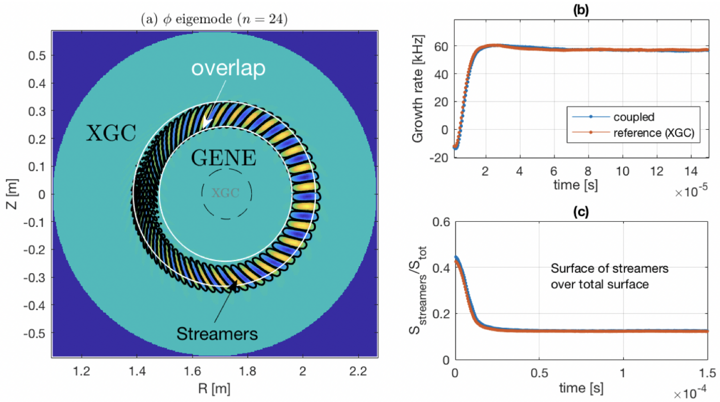

[J. Dominski et al., Exscale Computing Project meeting, Knoxville TN, March 2018]

1.3 GENE-XGC coupled simulation: Cyclone benchmark

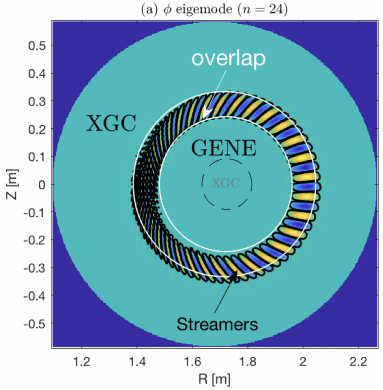

Linear benchmark

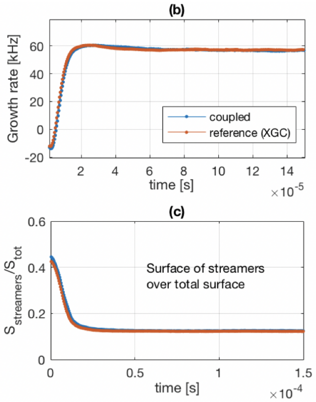

Nonlinear benchmark

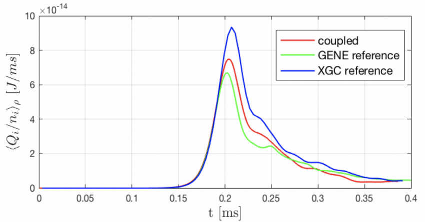

Very good agreements are found.

[J. Dominski et al., Exscale Computing Project meeting, Knoxville TN, March 2018]

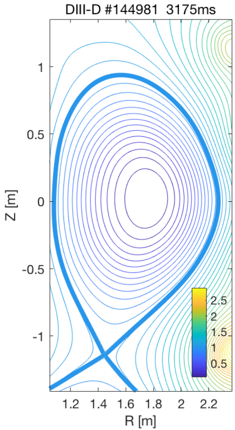

Linear benchmark

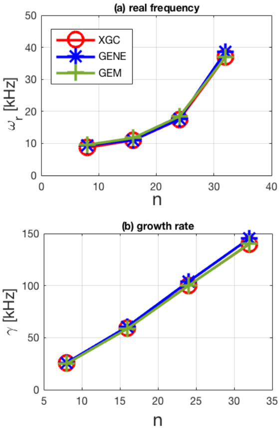

Nonlinear benchmark

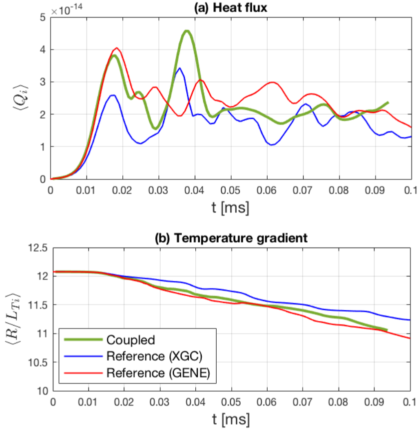

A very good agreement is found, given the difficulty of grid to grid transfer with this shaped geometry and the use of strong gradients (3× CBC) that excite short scales (in NL regime).

Conclusion of 1.

- We have a numerical scheme for coupling two gyrokinetic codes with minimal data exchange, well within allowable error bound (experiment).
- We have developed a technique for grid to grid interpolation. It will be improved by specialist (Mark Shephard, RPI).
- Exchange of additional information might be considered for some other cases. ADIOS is adapted to massive communications (like f).
- Option of using a particle core code (GEM) could help generalize our coupling approach and manage risk.

2. Impurities in XGC.

2.1 Verification of neoclassical physics with impurities.

2.2 The total-f gyrokinetic neoclassical version of XGC is used to study the baseline transport physics of model whole-volume JET H-mode plasmas under tungsten contamination.

Unlike other studies, separatrix and X-loss physics, non-Maxwellian pedestal, and electric field are calculated self-consistently.

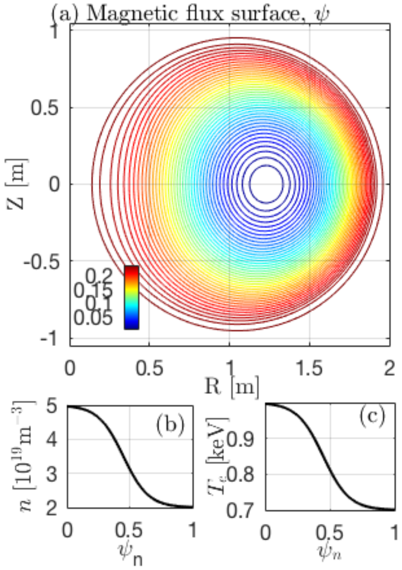

Neoclassical physics is verified with

- Full-f non-Maxwellian Fokker-Planck collisions. [Yoon-Chang PoP 2014] [Hager JCP 2016] and ES Yoon recently upgraded it to multi-species.
- Gyrokinetic ions and drift-kinetic electrons
- Axis-symmetric field solve ($n = 0$ and all m)

A very good agreement is found if the same Coulomb logarithm is used.

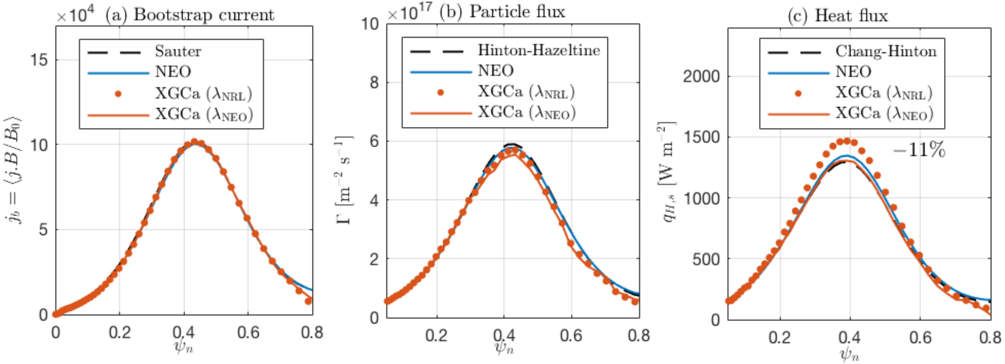

As a test, two identical species are used for modeling the deuterium in XGC.

2.1 Verification of an impure plasma

Various impure plasma are simulated. Impurities represents 1% of electron charge.
A very good agreement is found.

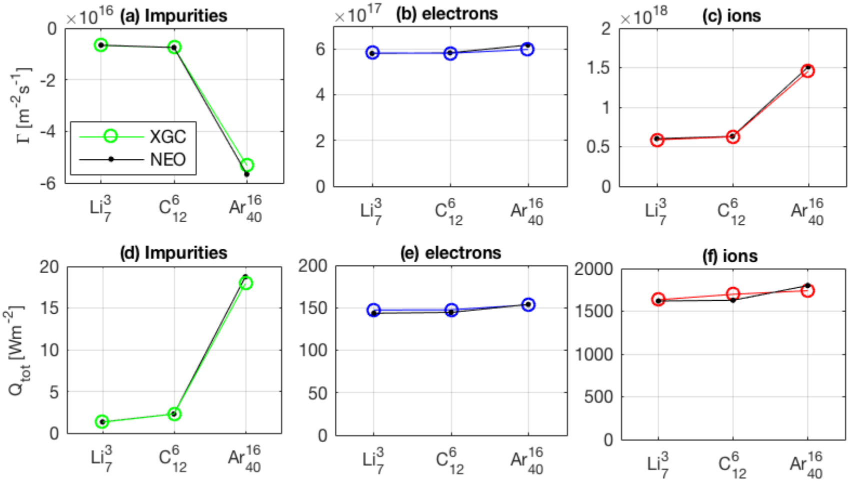

- A very good agreement is also found with NEO when using the same definition of the Coulomb logarithm.
- A very good agreement between XGCa and analytic estimates of particle flux, heat flux, and bootstrap current with the pure plasma.
- Very good agreement is found when injecting impurities in the plasma.
- The electron particle flux is weakly affected by impurities.

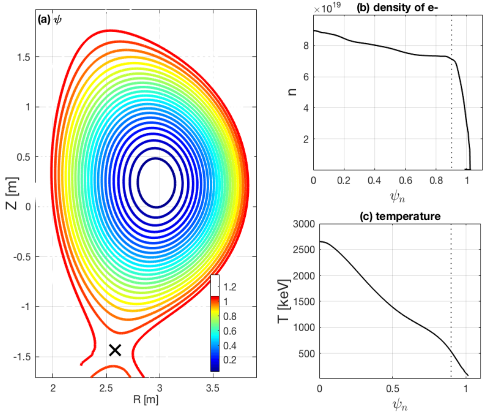

Neoclassical physics is studied with

- JET-like test case.
- Gyrokinetic deuterium and impurity species.
- Drift-kinetic electrons.
- Fokker-Planck non-Maxwellian multi-species collisions.
- Bundles of tungsten ionization states.
- $n_W/n_e \lesssim 10^{-4} \ll 1$: experimentally relevant.

- Low-Z penetrates the core and high-Z accumulates in the pedestal.

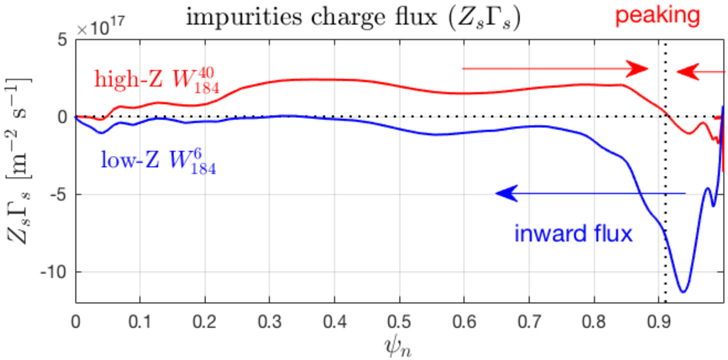

2.2 Z strongly influences the impurities particle flux

- Low-Z penetrates the core and high-Z accumulates in the pedestal.

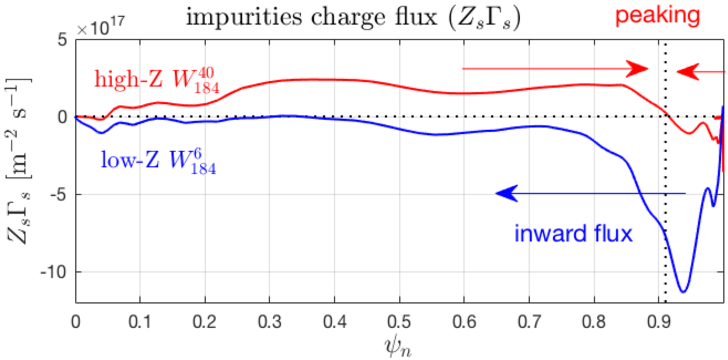

These results motivate a better model for the ionization stages of impurities.

2.2 $\langle Z \rangle$ is modeled with bundles (or super stages)

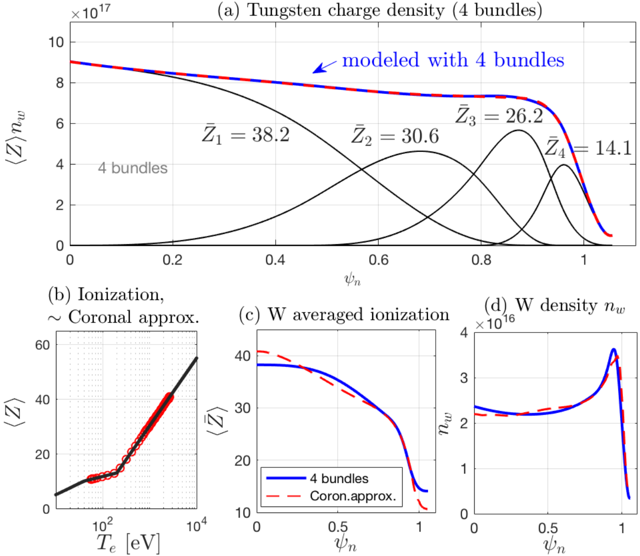

- The average charge state is taken from the Coronal approximation: $\langle Z \rangle = \langle Z \rangle (T_e)$, see (b).
- Bundles are build to fit this average charge state $\langle Z \rangle$ and a chosen impurities charge density ($n_w = 1\% \, n_e / \langle Z \rangle$).
- Atomic interactions are not yet implemented (work in progress).

2.2 Impurities flux requires realistic model of ionization stages

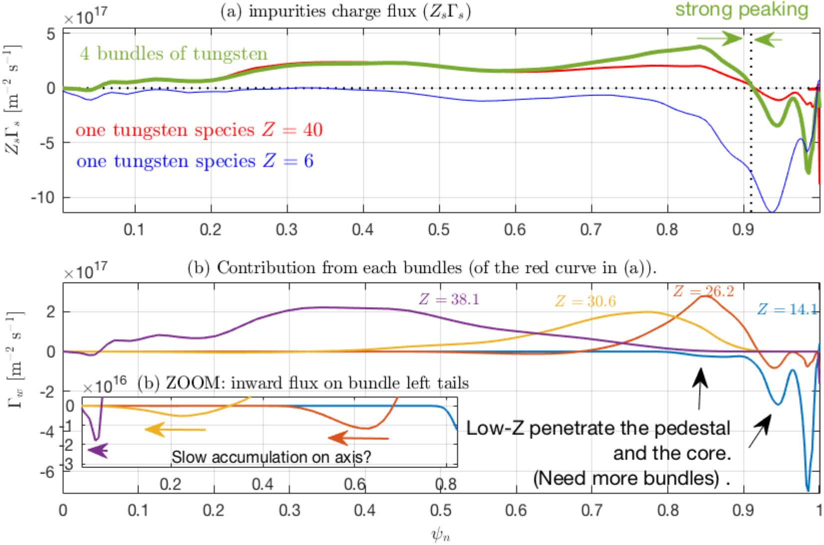

2.2 Poloidal asymetry depends on Z. Ongoing study.

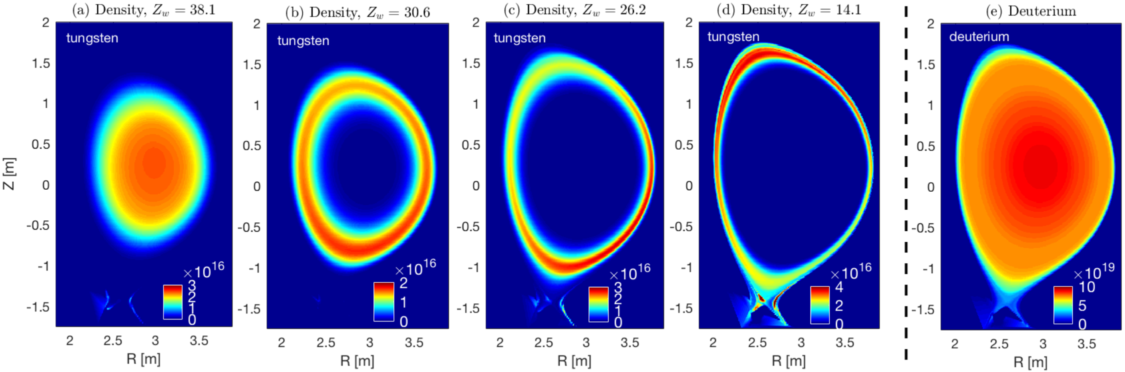

- Perturbation δn is of the order of background n_0 for impurities.
- T is actually compensating for n, s.t. $P = nT$ has less poloidal structure.
- I obtain similar poloidal structure when using only one impurity.
- Poloidal phase (up-down/down-up) is correlated with sign of particle flux (in/out).

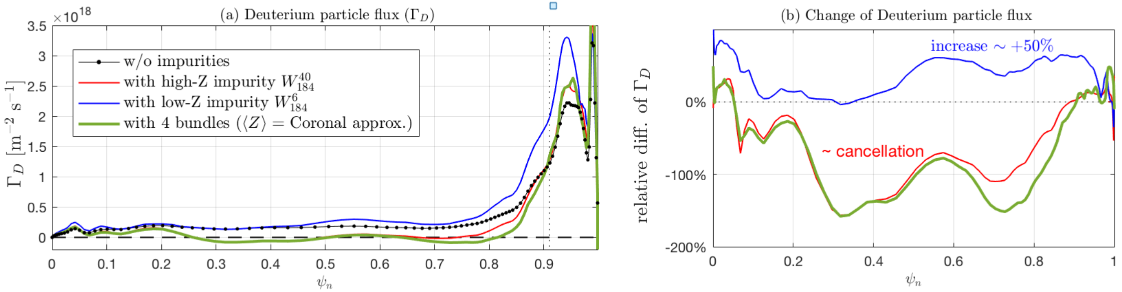

- Main ions compensate for tungsten particles flux (similar observation during verification exercise).
- (Electron particle flux is almost untouched (5%).)

2.2 Influence of impurities on ion fluxes

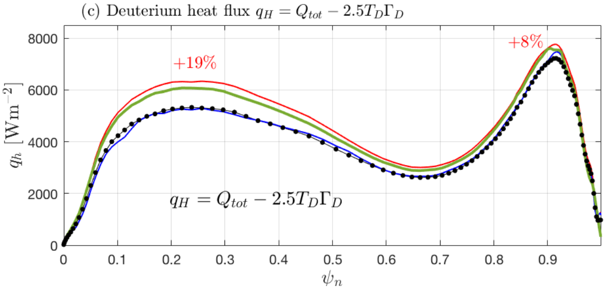

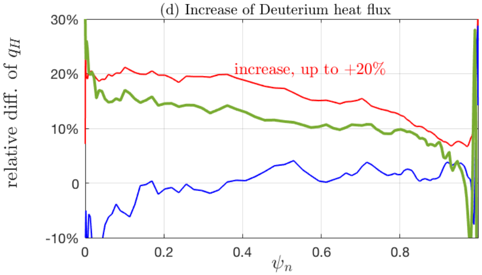

- Heat flux increased by high-Z ion/tungsten collisions. $\nu \propto n_Z Z^2 = (n_Z Z)Z$, s.t. high-$Z$ leads to higher collision frequency with main ions at $n_Z Z = cst$ (with $Z = 40$ one has $Z_{\text{eff}} = \sum_I n_I Z_I^2/n_e = 0.99 + 0.4 = 1.39$ and with $Z = 6$ one has $Z_{\text{eff}} = 1.05$).
- The convective contribution is smaller than the diffusive one.

2.3 Atomic processes: ionization/recombination

A missing element of the current model is the atomic process that changes the density of ionization states of an impurity.

Atomic collisions of impurities with electrons are most likely to dominate the processes at play.

- Recombination ($k > 0$ and $l > 0$): $W^{k+} + le^- \rightarrow W^{(k-l)+} + \hbar\nu\,(\text{radiation})$
- Ionization ($k < l$): $W^{k+} + e^- \rightarrow W^{l+} + \underbrace{e^-}_{\text{(hot from LHS)}} + \underbrace{(l-k)\,e^-}_{\text{(cold from ionization)}}$

Sputtering of tungsten from the wall will be studied in a second step, as it needs long simulation to be consistent.

In XGC the distribution function is represented with $f = f_a + f_g + f_p$, where

- f_a is an analytic Maxwellian initial function,
- f_g contains the slow (non Maxwellian) relaxation component and is represented on grid,
- f_p contains the rapid fluctuations and is represented with marker particles.

The slow atomic processes are being currently implemented on the grid component, f_g.
An atomic process modifying the ionization state l from state k could be described with probabilities $\mathcal{P}^{k\to l}$

$$\Delta f_g^{W^l} = \sum_k \mathcal{P}^{k\to l} \; f_g^{W^k}$$

and would require a modification of the electron charge density $(-n_e)$, through

$$\Delta n_e = \int dv \sum_k (l-k)\mathcal{P}^{k\to l} \; f_g^{W^k}.$$

2. Impurities in XGC

Achievements:

- Implemented and verified multi-species (gyrokinetic ions) in XGCa.
- Modeling the various ionization states of tungsten (W) with several bundles, in a XGCa simulation of the JET whole-device plasma including SOL.
- Whole-device neoclassical simulations of JET-like plasma show that low-Z tungstens penetrate the pedestal when high-Z tungstens are going out of the core.
- An accumulation of tungsten in the pedestal is found.

Ongoing and future works:

- Include turbulence.
- Implementation of atomic physics: ion recombination/ionization.
- Implement strong flows for heavy impurities.

3. Vision for the incoming years

Exascale must be used to allow us new discoveries where massive computations are key to produce early science results based on first-principles modeling.

W and Be impurities relevant for ITER is a perfect match for XGC studies.

- Penetration of tungsten through/in JET pedestal.
- Effect of W and Be on confinement.
- Why do low-Z impurity species improve confinement?
- Collapse of a pedestal due to radiations.

This would require or take advantage of new developments.

- Work on time projection and core-edge coupling.
- Optimize XGC for future architecture.
- Implementation of strong flows GK for impurities.